PROCEEDINGS OF SPIE

SPIEDigitalLibrary.org/conference-proceedings-of-spie

Dynamic calibration of a channeled spectropolarimeter for extended temperature stability

Chrysler, Benjamin, Otani, Yukitoshi, Hagen, Nathan

Benjamin D. Chrysler, Yukitoshi Otani, Nathan Hagen, "Dynamic calibration of a channeled spectropolarimeter for extended temperature stability," Proc. SPIE 11132, Polarization Science and Remote Sensing IX, 111320P (6 September 2019); doi: 10.1117/12.2528078

SPIE.

Event: SPIE Optical Engineering + Applications, 2019, San Diego, California, United States

Dynamic calibration of a channeled spectropolarimeter for extended temperature stability

Benjamin D. Chrysler[*a], Yukitoshi Otani[b], Nathan Hagen[b]

[A]University of Arizona, College of Optical Sciences, 1630 E. University Blvd., Tucson, Arizona 85721, USA; [B]Utsunomiya University, Center for Optical Research and Education, 7-1-2 Yoto, Utsunomiya, Tochigi, 321-8585 Japan

ABSTRACT

Channeled Spectropolarimeters (CHSP) are compact optical instruments that have potential for making precise polarization measurements without any moving parts. While most spectropolarimeters use rotating elements to make measurements, CHSPs use mechanically fixed thick retarders to modulate the Stokes vector onto the spectrum of light. In realistic applications, CHSPs must have calibration algorithms that give stable measurements in a variety of environmental conditions. Previous researchers developed a self-calibration algorithm that uses redundant channel information to compensate temperature-induced phase fluctuations in real-time without any additional reference measurements. In this paper we discuss the stability of the self-calibration technique. We identify a mathematical ambiguity in the algorithm that limits the range of temperatures over which the algorithm is stable. For a 60λ:120λ channeled spectropolarimeter with quartz retarders, the stable temperature range is only 27 ºC and is not suitable for many applications outside of the laboratory. We propose and demonstrate a modified algorithm that uses the slope of the phase to remove the mathematical ambiguity and extend the temperature range of the system. The demonstration shows stable operation over a 41 ºC temperature range and shows promise for increasing stability over a temperature range suitable for extreme terrestrial conditions.

Keywords: spectropolarimetry, polarimetry, signal processing, temperature stability, retarder, Stokes Vector

1. INTRODUCTION

Polarimeters are important optical instruments that have a range of applications[1] in astronomy, remote sensing, material science, biology, and the semiconductor industry. Polarimeters have the ability to measure the polarization of incoherent light which is represented by the Stokes vector. Spectropolarimeters are polarimeters that have the additional capability of measuring the spectral dependence of the Stokes vector, yielding additional information about the object being studied.

Most spectropolarimeters, including the commercially available Axoscan[2], use a rotating retarder in combination with polarizing optics to measure the Stokes vector[3,4]. Although this approach is the most widely used, it tends to be bulky, slow, and the use of rotating elements allows the possibility of mechanical breakdown. Another approach that has been studied is the snapshot channeled spectropolarimeter[5]. In this system, a set of mechanically fixed thick retarders are used instead of rotating elements. Channeled spectropolarimeters (CHSP) have the advantage of being compact, mechanically robust, and fast.

One of the key challenges for CHSPs is the development of a robust and accurate calibration scheme[6,7]. Calibration is necessary due to the use of thick retarders that are sensitive to environmental conditions such as temperature. Temperature changes of just several degrees can cause a significant change in the birefringence and result in phase changes on the order of a wavelength. CHSP instruments deployed outdoors in terrestrial conditions should operate over a wide temperature range, such as -40º C to 100º C in order to provide good performance in ranging from cold extremes in the arctic to

Polarization Science and Remote Sensing IX, edited by Julia M. Craven, Joseph A. Shaw, Frans Snik, Proc. of SPIE
Vol. 11132, 111320P · © 2019 SPIE · CCC code: 0277-786X/19/$21 · doi: 10.1117/12.2528078

temperature levels reached when exposed to direct sunlight for long periods of time. Operation over this temperature range should be sufficient for . Extraterrestrial systems may require even wider temperature ranges. Researchers developed a dynamic, or "self-calibrating" technique that uses redundant information in the spectrum to compensate for temperature-induced phase changes in real-time[8-10].

In this paper we discuss the stability of the self-calibration technique. We identify a mathematical ambiguity that occurs during phase-unwrapping and results in erroneous Stokes vector measurements when the temperature exceeds a threshold limit. We develop a theory to predict the temperature range in which a CHSP is stable based on the characteristics of the thick retarders. We propose an extended temperature range algorithm that uses the slope of the phase measured in the self-calibration algorithm to remove the phase ambiguity and improve stability. We demonstrate the existence of the self-calibration instability and show the ability of the extended range algorithm to increase the stability over a larger temperature range.

2. CHANNELED SPECTROPOLARIMETER

A CHSP consists of two thick retarders R_1 and R_2 and an analyzer A as shown in Fig. 1a. The fast axis of R_1 and the transmission axis of A define the measurement axis. The fast axis of R_2 is aligned at 45° with respect to the measurement axis. The retarder thicknesses are typically selected with a ratio $T_1/T_2 = 2$ or 3. Light with an arbitrary Stokes vector $\vec{S}(\sigma) = [S_0(\sigma) \quad S_1(\sigma) \quad S_2(\sigma) \quad S_3(\sigma)]^T$ illuminates the CHSP and is measured by a spectrometer, generating a signal[5] $P(\sigma)$:

$$P(\sigma) = \frac{1}{2}S_0(\sigma) + \frac{1}{2}S_1(\sigma)\cos\big(\phi_2(\sigma)\big) + \frac{1}{2}S_2(\sigma)\sin\big(\phi_2(\sigma)\big)\sin\big(\phi_1(\sigma)\big) - \frac{1}{2}S_3(\sigma)\sin\big(\phi_2(\sigma)\big)\cos\big(\phi_1(\sigma)\big). \quad (1)$$

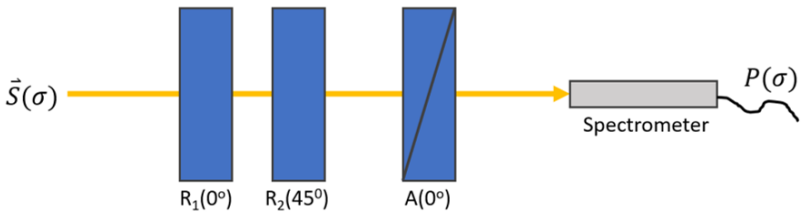

(a)

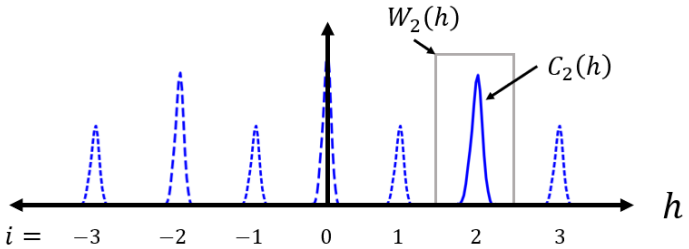

(b)

Figure 1: (a) Schematic of a channeled spectropolarimeter. Retarders R_1 and R_2 and analyzer A modulate the input Stokes Vector. The spectrum is measured by the spectrometer as $P(\sigma)$. (b) The Fourier transform of $P(\sigma)$ as a function of OPD, h, is depicted as the dotted

blue line. The channel numbers are indicated by i, the windowing function for the second channel $W_2(h)$ is depicted by the grey line, and the second channel $C_2(h)$ is depicted as the solid blue line.

The signal is divided into a set of channels $C_i(h)$ in the OPD domain by taking the Fourier transform of $P(\sigma)$ and multiplying by a windowing function $W_i(\sigma)$ as seen in Fig. 1b:

$$C_i(h) = \mathcal{F}\{P(\sigma)\} \cdot W_i(h), \tag{2}$$

Where OPD is represented as h and the windowing function is centered around the i[th] channel $C_i(h)$. Channel content $F_i(\sigma)$ in wavenumber space is determined by taking the inverse Fourier transform:

$$F_i(\sigma) = \mathcal{F}^{-1}\{C_i(h)\}, \tag{3}$$

The individual channel content is related to the Stokes vector components:

$$F_0(\sigma) = \tfrac{1}{2} S_0(\sigma),$$

$$F_1(\sigma) = \tfrac{1}{8} S_{23}^*(\sigma) \exp(j[\phi_2(\sigma) - \phi_1(\sigma)]),$$

$$F_2(\sigma) = \tfrac{1}{4} S_1(\sigma) \exp(j[\phi_2(\sigma)),$$

$$F_3(\sigma) = -\frac{1}{8} S_{23}(\sigma) \exp(j[\phi_2(\sigma) + \phi_1(\sigma)]), \tag{4}$$

where $S_{23}(\sigma) = S_2(\sigma) + jS_3(\sigma)$. In order to reconstruct the Stokes vector, the factors $K_i(\sigma)$ must calibrated. These factors compensate for the phase the of the thick retarders, as well as the amplitude and phase of the transfer function of the spectrometer itself. Processes for obtaining these factors are described in detail in this paper. The full Stokes vector can now be reconstructed using the 0[th], 2[nd] , and 3[rd] channels after calibrating the factors $K_i(\sigma)$:

$$\vec{S}(\sigma) = \begin{pmatrix} F_0(\sigma) \cdot K_0(\sigma) \\ F_2(\sigma) \cdot K_2(\sigma) \\ Re\{F_3(\sigma) \cdot K_3(\sigma)\} \\ -Im\{F_3(\sigma) \cdot K_3(\sigma)\} \end{pmatrix}, \tag{5}$$

Each calibration factor can be written as the product of a reference calibration factor $K_{r,i}(\sigma)$ representing the initial state of the system and a differential calibration factor $K_{d,i}(\sigma)$ representing the deviation from the initial state caused by perturbations such as temperature change:

$$K_i(\sigma) = K_{r,i}(\sigma) \cdot K_{d,i}(\sigma). \tag{6}$$

$K_{r,i}(\sigma)$ needs to be calibrated during the initial setup of the CHSP to determine the phase of the thick retarders. We use a reference beam approach similar to the one described in reference 9 to obtain $K_{r,i}(\sigma)$. $K_{d,i}(\sigma)$ needs to be continuously calibrated to compensate for phase changes in the thick retarders due to temperature fluctuations. In section 3 a self-calibration algorithm for obtaining $K_{d,i}(\sigma)$ is described and analyzed. In section 4, the self-calibration algorithm is modified to provide a more stable measurement of $K_{d,i}(\sigma)$ over a wide range of environmental temperature conditions.

3. SELF-CALIBRATION

The "self-calibration" technique uses redundant information given in the channels to determine the differential calibration factors $K_{d,i}(\sigma)$ and compensate fluctuations in the phases $\phi_1(\sigma)$ and $\phi_2(\sigma)$ of the thick retarders. After summarizing the technique as described in references 8,9 we identify a mathematical ambiguity in the phase-unwrapping procedure that results in instability of the self-calibration algorithm. We provide an analysis to determine the temperature range in which the instrument has stable operation.

3.1 Self-calibration algorithm

The difference in phase retardance between the reference measurement and the current measurement $\delta\phi_1(\sigma)$ and $\delta\phi_2(\sigma)$ for the two retarders are required to find $K_{d,i}(\sigma)$ and compensate for phase fluctuations in real-time. We use the self-calibration equations[8] to determine the phase of R_2 during the reference measurement $\phi_{2,r}(\sigma)$ and the phase of R_2 during the current measurement $\phi_{2,m}(\sigma)$:

$$\tan\left(2\cdot\phi_{2,r}(\sigma)\right) = K_{2,r}(\sigma)^2 + K_{1,r}(\sigma)\cdot K_{3,r}(\sigma) \tag{7}$$

$$\tan\left(2\cdot\phi_{2,m}(\sigma)\right) = F_2(\sigma)^2 + F_1(\sigma)\cdot F_3(\sigma) \tag{8}$$

Due to tangent function, the phases must be unwrapped. As a result, the phases can only be determined within an integer number of 2π accuracy. After dividing the unwrapped phase by 2, the measured phase functions of the reference and current measurement $\theta_{2,r}(\sigma)$ and $\theta_{2,m}(\sigma)$ are:

$$\theta_{2,r}(\sigma) = \phi_{2,r}(\sigma) + n_r\pi = \frac{1}{2}\mathrm{UNWRAP}\left\{\tan^{-1}\left[K_{2,r}(\sigma)^2 + K_{1,r}(\sigma)\cdot K_{3,r}(\sigma)\right]\right\} \tag{9}$$

$$\theta_{2,m}(\sigma) = \phi_{2,m}(\sigma) + n_m\pi = \frac{1}{2}\mathrm{UNWRAP}\{\tan^{-1}[F_2(\sigma)^2 + F_1(\sigma)\cdot F_3(\sigma)]\} \tag{10}$$

Where n_r and n_m are integers. The difference between the two measured phase functions yields the measured phase difference, $\delta\theta_2(\sigma)$:

$$\delta\theta_2(\sigma) = \theta_{2,m}(\sigma) - \theta_{2,r}(\sigma) = \delta\phi_2(\sigma) + n\pi \tag{11}$$

Thus, the measured phase difference $\delta\theta_2(\sigma)$ is known within $n\pi$ accuracy of the actual phase difference $\delta\phi_2(\sigma)$ where n is an integer. The differential phase retardance of R_1, $\delta\phi_1(\sigma)$, can be determined if the ratio ρ of the thicknesses of the two retarders are known:

$$\rho = \frac{\phi_2(\sigma)}{\phi_1(\sigma)} = \frac{T_2}{T_1} \tag{12}$$

The retardance $\delta\phi_1(\sigma)$ can be determined within $n\pi/\rho$ accuracy:

$$\delta\phi_1(\sigma) = \frac{\delta\theta_2(\sigma)}{\rho} - \frac{n\pi}{\rho} \tag{13}$$

And the differential calibration coefficients are determined:

$$K_{1,d}(\sigma) = \exp[j\left(1-\frac{1}{\rho}\right)(\delta\theta_2(\sigma) - n\pi)]$$

$$K_{2,d}(\sigma) = \exp[j(\delta\theta_2(\sigma) - n\pi)]$$

$$K_{3,d}(\sigma) = \exp\left[j\left(1+\frac{1}{\rho}\right)(\delta\theta_2(\sigma) - n\pi)\right] \tag{14}$$

3.2 Phase-unwrapping

Phase-unwrapping algorithms must have a phase reference since only relative changes in phase can be determined and the absolute phase cannot be determined. Most phase-unwrapping algorithms will implicitly assign an initial phase reference in the range of $[0,2\pi)$ to the first wavenumber in the spectrum and then begin unwrapping the phase towards higher wavenumbers. If there is noise in the spectrum at the wavenumber where the phase reference is taken, the reconstructed phase may have errors that affect the Stokes vector reconstruction. Assuming that the phase-unwrapping function assigns the phase reference to the first wavenumber in the spectrum, the phase reference can be shifted to a different wavenumber σ_{ref} in a part of the spectrum that has higher signal-to-noise ratio using the following equation:

$$\theta'(\sigma) = \theta(\sigma) - 2\pi \cdot \text{floor}\left\{\frac{\theta(\sigma_{ref})}{2\pi}\right\} \tag{15}$$

where $\theta'(\sigma)$ is the phase function with the desired phase reference and $\theta(\sigma)$ is the phase function directly returned by the phase-unwrapping algorithm. The floor{}function rounds the argument down to the nearest integer.

3.3 Limitations of the self-calibration algorithm

In previous studies, researchers did not consider the phase ambiguity caused by the unknown integer n and implicitly assumed that $n = 0$. This assumption is true for small deviations from the reference phase, but if the phase deviation becomes large then $n \neq 0$. If the value of n is incorrectly chosen, the results of the Stokes reconstruction may be inaccurate. If in the self-calibration n is assumed to be 0, then the calibration factors will have a phase error $\epsilon K_{i,d}(\sigma)$:

$$\begin{aligned} \epsilon K_{1,d}(\sigma) &= \exp[-j\left(1 - \frac{1}{\rho}\right)n\pi] \\ \epsilon K_{2,d}(\sigma) &= \exp[-jn\pi] \\ \epsilon K_{3,d}(\sigma) &= \exp\left[-j\left(1 + \frac{1}{\rho}\right)n\pi\right] \end{aligned} \tag{16}$$

When n is assumed to be 0, the reconstructed Stokes vector $\vec{S}(\sigma)$ is represented in terms of the actual Stokes vector components S_0, S_1, S_2, S_3 and the actual value of n:

$$\vec{S}(\sigma) = \begin{pmatrix} S_0 \\ S_1 \cdot \cos(jn\pi) \\ S_2 \cdot \cos\left[j\left(1 + \frac{1}{\rho}\right)n\pi\right] + S_3 \cdot \sin\left[j\left(1 + \frac{1}{\rho}\right)n\pi\right] \\ S_3 \cdot \cos\left[j\left(1 + \frac{1}{\rho}\right)n\pi\right] - S_2 \cdot \sin\left[j\left(1 + \frac{1}{\rho}\right)n\pi\right] \end{pmatrix} \tag{17}$$

If the true value of n is 0, then the reconstructed Stokes vector will simplify to the actual Stokes vector and the measurement will be correct. However, if the phase has deviated significantly from the reference phase and the true value of n is non-zero, then the reconstructed Stokes vector will have error. S_1 will have a sign error for odd values of n and S_2 and S_3 will be reconstructed as a linear combination of the actual S_2 and S_3 components.

Next, we quantify the maximum deviation from the reference phase that produces accurate measurements when making the assumption $n = 0$. The phase of retarder R_2 at the reference wavenumber exists in the intervals $\theta_{2,r}(\sigma_{ref}) \ni [0, \pi)$ and $\theta_{2,m}(\sigma_{ref}) \ni [0, \pi)$ for both the reference and current phase measurements. When the actual value of $n = 0$ the phase difference $\delta\phi_2(\sigma_{ref})$ lies in the interval:

$$\delta\phi_2(\sigma_{ref}) \ni \left(-\theta_{2,r}(\sigma_{ref}), \pi - \theta_{2,r}(\sigma_{ref})\right] \tag{18}$$

Next, we find the temperature range over which the system is stable. The change in phase retardance due to a change in temperature is determined using the coefficient γ that is expressed as the normalized change in phase per unit change in temperature[11]. Through this coefficient the change in phase retardance is proportional to the change in temperature:

$$\delta\phi_2(\sigma_{ref}) = \gamma \cdot \phi_{2,r}(\sigma_{ref}) \cdot \Delta T \tag{19}$$

The temperature range over which a CHSP is stable can be expressed in terms of the temperature during reference calibration T_0 after rearranging for ΔT:

$$T \ni \left[T_0 + \frac{\pi - \theta_{2,r}(\sigma_{ref})}{\gamma \cdot \phi_{2,r}(\sigma_{ref})}, T_0 - \frac{\theta_{2,r}(\sigma_{ref})}{\gamma \cdot \phi_{2,r}(\sigma_{ref})}\right) \tag{20}$$

And the absolute temperature range over which the instrument is stable is:

$$\Delta T = \left| \frac{\pi}{\gamma \cdot \phi_{2,r}(\sigma_{ref})} \right| \tag{21}$$

While the measured reference phase $\theta_{2,r}(\sigma_{ref})$ is determined by measurement, the absolute reference phase $\phi_{2,r}(\sigma_{ref})$ cannot be determined directly. However, an approximate value can be used based on the specification of the retarder. A retarder specified with a number of waves of retardance WV at a specification wavelength λ_{spec} has a phase retardance:

$$\phi_{2,r}(\sigma_{ref}) = 2\pi \cdot WV \cdot \sigma_{ref} \cdot \lambda_{spec} \tag{22}$$

Although the absolute range over which the CHSP is stable is easily determined based on the materials and specifications of the thick retarders, the upper and lower temperature bounds are not symmetric around the initial temperature. Furthermore, the upper and lower bounds are essentially unpredictable since $\theta_{2,r}(\sigma_{ref})$ is not known until the reference measurement is taken. In the case that the reference phase happens to be close to the bounds 0 or π, the ability to withstand temperature increases or decreases may be severely limited.

As an example, consider a CHSP system with 60λ and 120λ retarders specified at λ_{spec} = 633nm and made out of quartz ($\gamma = -1.4 \cdot 10^{-4}[\frac{1}{\mathrm{K}}]$). For a reference wavenumber at $\sigma_{ref} = 1.72 \cdot 10^6$ The total temperature range of the system is 27.3 ^{o}C. If the initial phase at the reference wavenumber is $\theta_{2,r}(\sigma_{ref}) = .09\pi$ and the ambient temperature during the reference calibration is $T_0 = 21.0\,^{o}$C, then the stable temperature range is [-3.9 ^{o}C, 23.4 ^{o}C].

4. EXTENDED TEMPERATURE RANGE CALIBRATION

In this section we show that the temperature range of a CHSP instrument can be extended beyond the limitations described in section 3.3 by using the slope of the phase retardance to determine the value of *n*.

4.1 Extended Range Calibration Algorithm

First, we fit the measured reference phase $\theta_{2,r}(\sigma)$ and measured current phase $\theta_{2,m}(\sigma)$ to the linear approximations $\psi_m(\sigma) = \mathrm{A}_m\sigma + \mathrm{B}_m$ and $\psi_r(\sigma) = \mathrm{A}_r\sigma + \mathrm{B}_r$. We assume that the difference in phase between the reference and the current measurement $\delta\phi_2(\sigma_{ref})$ can be modeled using the slopes obtained in the linear fit:

$$\delta\phi_2(\sigma_{ref}) = \sigma_{ref}(\mathrm{A}_m - \mathrm{A}_r) \tag{23}$$

Using Eq. 14 and Eq. 26 we relate the measured slope differential and the linear fit coefficients to the measured phase difference $\delta\theta_2(\sigma_{ref})$ and the integer *n*:

$$\sigma_{ref}(\mathrm{A}_m - \mathrm{A}_r) = \delta\theta_2(\sigma_{ref}) + n\pi \tag{24}$$

Since the fit is an approximation and *n* must be an exact integer, we use a minimization function to find the value of *n* that best satisfies the equation:

$$\min_{\mathrm{n}}\{\sigma_{ref}(\mathrm{A}_m - \mathrm{A}_r) - [\delta\theta_2(\sigma_{ref}) + n\pi]\} \tag{25}$$

The correct value of *n* is then inserted into Eq. 17 for stable operation over a large temperature range.

5. EXPERIMENTAL RESULTS

A CHSP system was assembled as shown in Fig. 2 to demonstrate the temperature range limitations discussed in section 3.3 and to demonstrate the extended temperature range algorithm presented in section 4. The system uses a 60λ thick retarder oriented at 0^{o} and two 60λ retarders oriented at 45^{o}. The two retarders at 45^{o} effectively operate as a single 120λ retarder. A polarization state generator consists of a broadband halogen lamp and a polarization element. An Ocean Optics USB4000+ Spectrometer is used to measure the spectrum after the light passes through all the polarization components. The system is placed in an enclosed chamber and the temperature of the CHSP system is uniformly increased using a heat source in combination with a fan for air circulation.

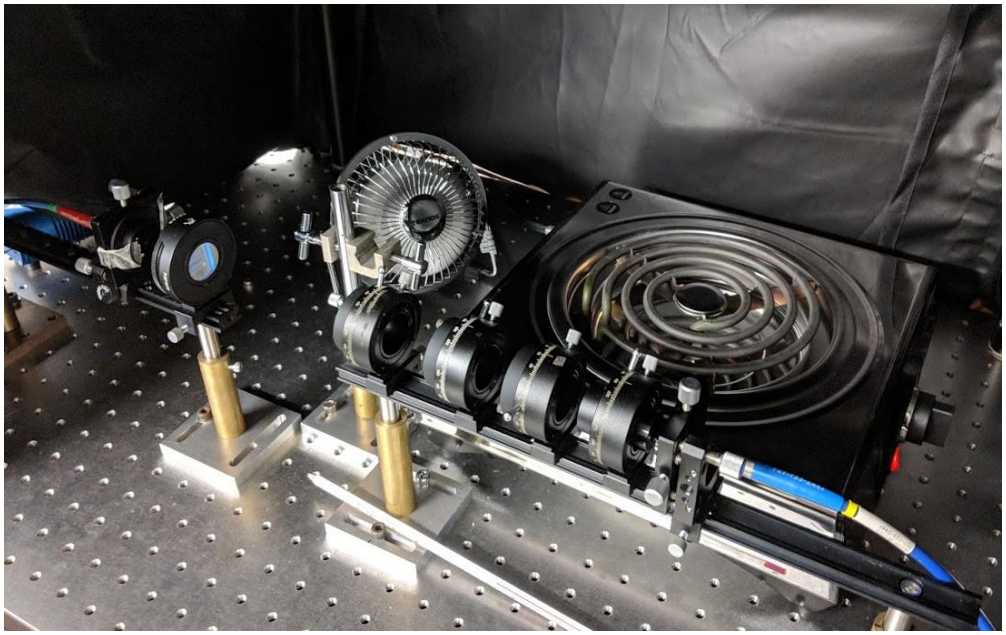

Figure 2: A demonstration CHSP system is assembled using 60λ quartz retarders. The retarders are arranged to effectively form a 60λ : 120λ CHSP. A broadband light source and a linear polarizer form a polarization state generator. The system is placed in a heating chamber with air flow to uniformly increase the temperature and observe its effect on stability.

In the experiment a linear polarizer oriented at approximately 22.5 degrees is used in the polarization state generator to produce a Stokes vector with nonzero S_1 and S_2 polarization but no S_3 polarization. The system was initially calibrated at an ambient temperature of 21 ºC using the reference light technique from reference 9. The temperature of the system was gradually increased from 21 ºC to 62 ºC and measurements were made at 14 different temperatures. The reconstructed Stokes vector components are spectrally averaged and plotted against temperature in Fig. 3a for the original self-calibration algorithm and in Fig. 3b for the extended temperature range algorithm.

The example at the end of section 3.3 has all the same parameters as this experiment and is used as a basis for comparison to theory. When we reconstruct the Stokes vector using the original self-calibration method we observe an abrupt change in the measured Stokes vector at around 25 ºC in the transition from $n = 0$ to $n = 1$. This agrees well with theory where we predict that the stable temperature range has an upper limit of 23.4 ºC. We also observe a second abrupt change during the transition from $n = 1$ to $n = 2$. This transition is observed to occur at 52 ºC in close agreement with the theoretical prediction of 50.7 ºC. Using the extended temperature range algorithm all abrupt changes in the Stokes vector are eliminated and the algorithm is demonstrated to be stable over a 41 ºC temperature range. The experiment also shows the algorithm can correctly predict n values of at least 2. Assuming the algorithm is stable for the entire range in which $n = 2$ then we can determine this system has a stable temperature range over 136.5 degrees ranging from -58.5 ºC to 78 ºC. If the algorithm continues to provide stable results for $n = 3$ then the system has potential to be stable even for extreme terrestrial conditions.

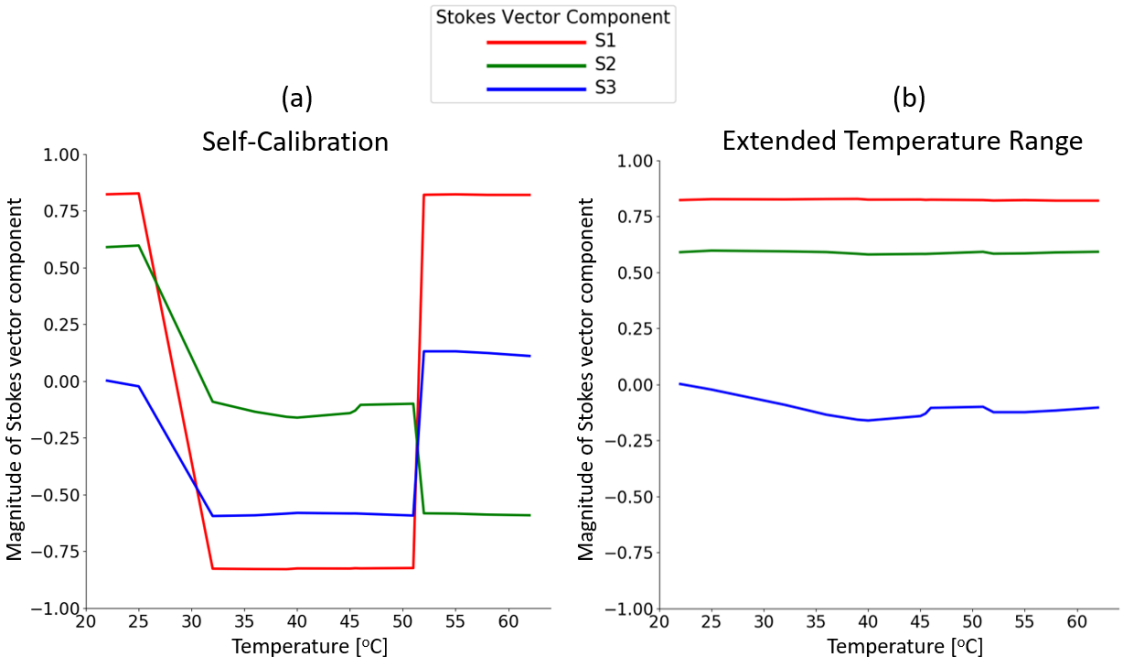

Figure 3: Stokes vector reconstruction as a function of temperature using different reconstruction algorithms. The sample was a linear polarizer oriented at approximately 22.5 degrees. Since the Stokes vector components from the linear polarizer do not vary with spectrum, they were averaged from 0.5um to 0.9um. (a) Reconstruction using the original self-calibration technique. Since the technique does not account for the changing value of n, the measurement abruptly changes at 25 °C and 52 °C. (b) Reconstruction using the extended temperature range algorithm provides stable measurements as temperature increases.

6. CONCLUSION

In this paper we discuss the stability of a real-time calibration technique for channeled spectropolarimeters. We find that a mathematical ambiguity in the technique results in a limited temperature range in which the system is stable. For a system that uses a pair of 60λ and 120λ quartz retarders the temperature range is limited to 27 °C and is not sufficient for applications outside the laboratory. We propose an extended temperature range algorithm that uses the slope of the phase obtained in the self-calibration algorithm to remove the mathematical ambiguity and extend the temperature range over which the system is stable. We demonstrate these claims by assembling a 60λ:120λ channeled spectropolarimeter and placing it in a heat-controlled chamber. After raising the heat in the chamber from 21 °C to 62 °C we observed abrupt changes in the reconstructed Stokes vector at 25 °C and 52 °C when using the original self-calibration algorithm, but did not observe any abrupt changes when using the extended temperature algorithm. The new algorithm has the potential to improve the stability of channeled spectropolarimeters over a broad temperature range.

7. ACKNOWLEDGEMENTS

We would like to acknowledge support from the National Science Foundation Graduate Research Opportunities Worldwide program, and the Japan Society for the Promotion of Science. Ben Chrysler would like to acknowledge support from the National Science Foundation Graduate Research Fellowship Program Grant (DGE-1143953). Any opinions, findings, and conclusions or recommendations expressed in this material are those of the authors and do not necessarily reflect the views of the National Science Foundation.

REFERENCES

[1] Goldstein, D.H., "Applications and limitations of polarimetry," Proc. SPIE 1317, 210-223 (1990).

[2] “AxoScan – Mueller Matrix Polarimeter,” Axometrics Inc. Retrieved 07/15/19 https://www.axometrics.com/products/axoscan

[3] Kawabata, K.S., Okazaki, A., Akitaya, H., Hirakata, N., Hirata, R., Ikeda, Y., Kondoh, M., Masuda, S., Seki, M., "A new spectropolarimeter at the Dodaira Observatory," Publ. Astron. Soc. Pac. 111(761), 898 (1999).

[4] Goldstein, D.H., "Mueller matrix dual-rotating retarder polarimeter," Appl. Opt. 31(31), 6676-6683 (1992).

[5] Oka, K., Kato,T, "Spectroscopic polarimetry with a channeled spectrum," Opt. Lett. 24(21), 1475-1477 (1999).

[6] Kudenov, M.W., Hagen, N.A., Dereniak, E.L., Gerhart, G.R., "Fourier transform channeled spectropolarimetry in the MWIR," Opt. Express 15(20), 12792-12805 (2007).

[7] Craven, J., Kudenov, M.W., "False signature reduction in channeled spectropolarimetry," Opt. Eng. 49(5) 053602 (2010).

[8] Taniguchi, A., Oka, K., Okabe, H., Hayakawa, M., "Stabilization of a channeled spectropolarimeter by self-calibration," Opt. Lett. 31(22), 3279-3281 (2006).

[9] Okabe, H., Hayakawa, M., Matoba, J., Naito, H., Oka, K.. "Error-reduced channeled spectroscopic ellipsometer with palm-size sensing head." Rev. Sci. Instrum. 80(8) 083104 (2009).

[10] Xing, W., Ju, X., Yan, C., Yang, B., Zhang, J., "Self-correction of alignment errors and retardations for a channeled spectropolarimeter," Appl. Opt. 57(27) 7857-7864 (2018).

[11] Hale, P. D., Day, G.W., "Stability of birefringent linear retarders (waveplates)," Appl. Opt. 27(24) 5146-5153 (1988).